CHEMIJA. 2021. Vol. 32. No. 3–4. P. 73–82

Design and applications of a neural networks assisted portable liquid surface tensiometer

Tomas Drevinskas[1],

Jūratė Balevičiūtė[1],

Kristina Bimbiraitė-Survilienė[1],

Gediminas Dūda[1],

Mantas Stankevičius[1],

Nicola Tiso[1], Rūta Mickienė[1],

Domantas Armonavičius[1],

Donatas Levišauskas[1, 2],

Vilma Kaškonienė[1],

Ona Ragažinskienė[3],

Saulius Grigiškis[4],

Enrica Donati[5],

Massimo Zacchini[5],

Audrius Maruška[1*]

[1] *Instrumental Analysis Open Access Centre, Faculty of Natural Sciences, Vytautas Magnus University, 8 Vileikos Street, 44404 Kaunas, Lithuania*

[2] *Process Control Department, Kaunas University of Technology, 50 Studentų Street, 51368 Kaunas, Lithuania*

[3] *Kaunas Botanical Garden of Vytautas Magnus University, 6 Ž. E. Žilibero Street, 46324 Kaunas, Lithuania*

[4] *JSC Biocentras, 29 Šiltnamių Street, 14117 Pagiriai, Lithuania*

[5] *National Research Council, Area della Ricerca di Roma, via Salaria Km 29.300-00015, Monterotondo (Rome), Italy*

In this paper, a portable instrument for surface tension measurements, characterization and applications is described. The instrumentation is operated wirelessly, and samples can be measured *in situ*. The instrument has changeable different size probes; therefore, it is possible to measure samples from 1 ml up to 10 ml. The response of the measured retraction force and the concentrations of measured surfactant is complex. Therefore, two calibration methods were proposed: (i) the conditional calibration using polynomial and logarithmic fitting and (ii) the neural network trained model prediction of the surfactant concentration in samples. Calibrating the instrument, the neural network trained model showed a superior coefficient of determination (0.999), comparing it to the conditional calibration using polynomial (0.992) and logarithmic (0.991) fit equations.

Keywords: liquid surface tension, portable, instrumentation, environmental analysis, bioanalysis, neural networks

* Corresponding author. Email: audrius.maruska@vdu.lt

INTRODUCTION

Portable and autonomous analytical instrumentation offers multiple advantages. The advantages are the following: (i) *in situ* as well as in laboratory measurement, (ii) easy transportation, (iii) no need of additional devices, (iv) small dimensions and weight, (v) wireless operation, (vi) possible use in a hazardous environment, (vii) possible integration in another analytical systems and production lines, and (viii) independent or unattended measurement [1].

The developed portable and autonomous analytical instruments are related to the following techniques: separation, electrochemistry, photometry, spectroscopy and spectrometry [2–6]. In some cases, special data ordering and analysis methods interpret chemometric data. Therefore, the imperceptible features can be riddled out, like it was demonstrated identifying the antiviral substances in the crude plant extracts [7]. Also, an extraction recovery was predicted from chemometric data using a combination of a mathematical model and a machine learning method [8]. Some physicochemical properties such as liquid surface tension are a product of multiple chemical substances. And therefore, it cannot be measured by separation techniques or mass spectrometry.

Surface tension modifying substances, commonly called surface-active materials, are considered toxic to the organisms living in the water [9]. It is also known in the literature that the monolayer of surfactant on the water surface prevents oxygen exchange [10, 11]. Multiple cases report wastewaters contaminated by detergents [12]. Additionally, some proteins, oligopeptides and enzymes are known for their surface tension modifying properties. In the previous investigations, white-rot fungi – *Irpex lacteus* – reduced the surface tension of the growth medium. The fungi also degraded a significant amount of anthracene which only dissolves in surfactant-containing water [13]. Consequently, the need for portable and autonomous surface tension measurement systems is undoubted. Combining such instruments with a machine learning method is expected to provide better information on the investigated features.

The aim of this work is to characterize the developed miniaturized portable liquid surface measurement instrumentation and apply it for real sample investigations *in situ*.

EXPERIMENTAL

Chemicals

Acetone (99.9%) and methanol (99.9%) were from Macron (Poland). Malt extract and sodium dodecyl sulfate (SDS) (>99.0%) were purchased from Roth (Germany). *Pleurotus ostreatus* (*P. ostreatus*) and *Irpex lacteus* (*I. lacteus*) were isolated and confirmed in the previous studies [14]. Bidistilled water was produced in the laboratory using a Fistreem Cyclon bidistillator (UK).

Sample preparation

For measurement standards, stock solutions were prepared: the required amount of chemical substance was dissolved in 15 ml of bidistilled water and kept in a freezer at –20°C. Before further use, the stock solutions were defrosted and used for preparing the required levels of concentrations. At least ten different levels of concentrations were used for each compound.

The fungi were grown in a miniaturized format according to the previously optimized procedure [13]. In a 10 ml gas chromatography vial, 2.5 ml of the growth medium (0.6% malt extract) was added. Instead of septa in the vial seal, a cotton disc was used to ensure the gas exchange. 0.03 g of fungi was added to the growth medium in the vial and incubated at room temperature c.a. 22°C. After 17 days of growing when the fungi reached the plateau region, measurement of the medium was performed. The growth medium was diluted two times so that 4 ml of measurement solution would be obtained.

For the modelling and determination of residual detergents on the surfaces the following procedure was used: (i) 2 ml of 10 mM concentration SDS in methanol was added onto the (a) stainless steel and (b) glass, (ii) after the evaporation of methanol, (iii) 4 ml of bidistilled water was added onto the application site of the surfactant, (iv) left for 15 min for extraction and (v) 4 ml of water with the dissolved surfactant from the surface was added to the measurement vial and measured.

In situ determination of river water

The selected sites of the rivers Neris (coordinates: 54°53'57.2"N 23°52'34.4"E) and Nemunas (coordinates: 54°53'50.5"N 23°52'34.7"E) were sampled taking 4 ml of river water and directly used for

the measurement. Each measurement was repeated five times, and the mean was used as the determining retraction force value, which later was recalculated to the equivalent SDS concentration.

Portable liquid surface tensiometer and measurement procedures

The instrument for measuring the surface tension was developed according to the previously published paper, where similar mechanics and electronics were used for the measurement of the hardness of Actinidia fruit peel [15]. A schematic diagram of portable measurements is represented in Fig. 1.

The sketches of measurement probes were designed using Inkscape – the open-source vector graphics editor software (https://inkscape.org/). The sketches were processed using KiCad – the open-source electronics design software (http://kicad-pcb.org/). The processed sketches of the probes were manufactured by the printed circuit board production company SEEED (PRC). The copper of measurement probes was tin-plated.

The measurement principle is the following: (a) the vial with the sample (4 ml) is placed on the lifting platform in the instrument, (b) the sample is lifted up, (c) upon the lift up, the force sensor is auto-zeroed, (d) the platform with the sample is lifted down at the selected speed, (e) during the lifting down, the force is measured, (f) the maximum value of the force reading is considered as the value of the surface tension and is sent wirelessly to the control interface (smartphone, laptop, table pc, etc.). For more sensitive readings of the surface tension, the previously developed migration velocity-adaptive moving average method was modified to suit the surface tension measurements [16].

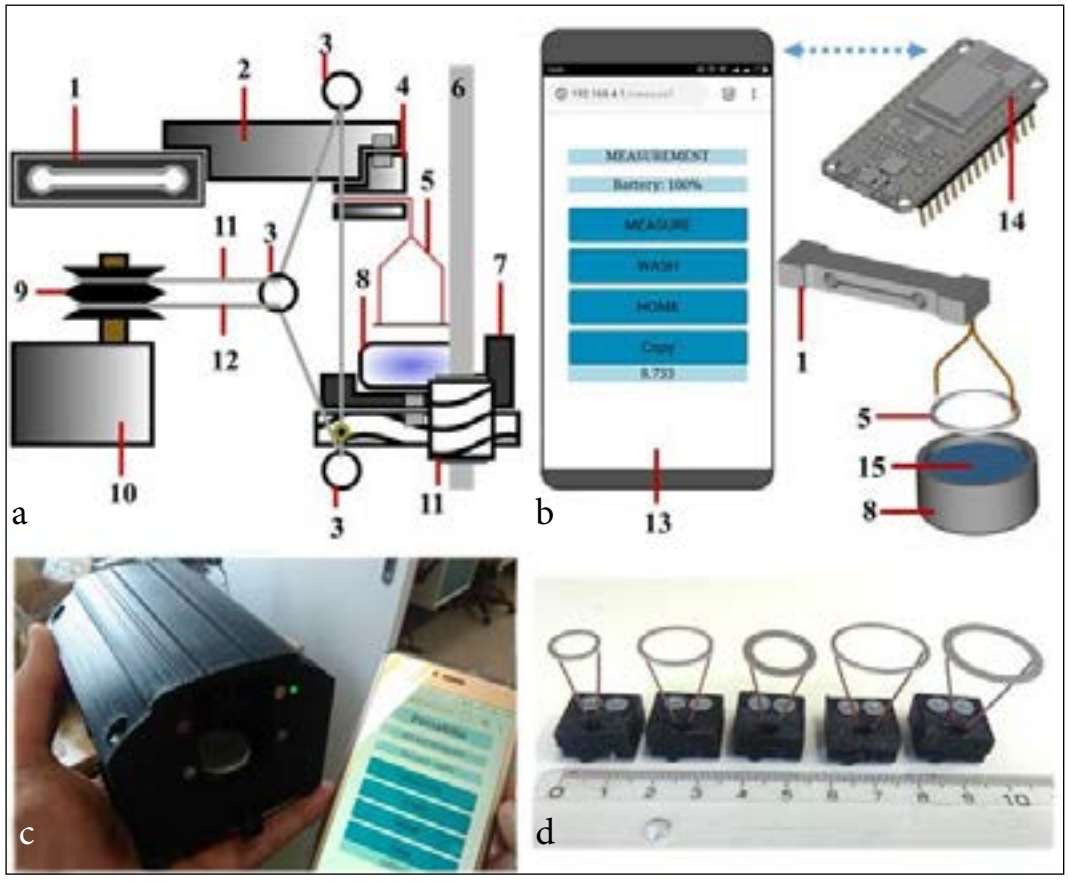

Fig. 1. Designed portable surface tension measurement instrument. (a) A schematic design diagram, (b) the principle of measurement, (c) an actual photograph of the instrument and (d) a photograph of the measurement probes. Markings: 1, force sensor; 2, sensitivity enhancement lever; 3, thread guiding loops; 4, probe adapter; 5, measurement probe; 6, vertical guiding shaft; 7, vial seat; 8, sample vial; 9, thread spool; 10, stepper motor; 11, upper thread; 12, lower thread; 13, smartphone; 14, microcontroller; 15, liquid sample

Between the measurements of different samples, the probes were washed, immersing them into bidistilled water five times.

Data analysis

Means of the measured force, standard deviation and relative standard deviation were calculated, and polynomial and logarithmic curves of the measured force were fit against the equivalent concentration of SDS using the Microsoft Excel software. For the neural network (NN) models, the data was normalized using the mathematical Rstudio software [17]. The NN models were calculated, and predictions were performed using the R-package neuralnet [18]. The NN models were generated using two procedures.

The first NN procedure. All measured force values representing surface tension for the calibration of SDS were treated as separate data points. Totally 140 data points (14 different levels of concentrations in a range of 0.005 and 21.672 μM, 10 repetitions for each level) were used for the generation of the NN model.

The second NN procedure. Similar to polynomial and logarithmic curve fitting, means of the measured force were used. Neural networks are a type of machine learning method that only works effectively with large data sets, and 14 data points (means) were not enough for the satisfactory model. Knowing the relative standard deviation (<2.5%) for the mean of the measured force of a concentration level, additional data points were generated, injecting the errors to the means and concentration levels similarly like it was described in previously published results [19, 20]. Totally 2,000 data points were generated and used for the calculation of the NN model.

Before calculating the NN model, the data were scaled so that the largest number was equated to 1 and the smallest number was equated to 0 following Eq. (1),

$$m_i = \frac{x_i - x_{\min}}{x_{\max} - x_{\min}}, i = 1, 2...I, \quad (1)$$

where m_i is the normalized value, i (i = 1, 2…I) is the record number in the data set (data table), x_i is the original value in the data set, $x_{\min}$ is the minimum value of the data set, and $x_{\max}$ is the maximum value of the data set. The data sets were separated into 2 equally sized segments – one for training the NN model and another for testing the generated NN model. For the characterization of NN models, the mean squared error (MSE) was calculated following Eq. (2),

$$MSE = \frac{1}{I}\sum_{i-1}^{I}(p_i - x_i)^2, i = 1, 2...I, \quad (2)$$

where MSE is the mean squared error, i (I = 1, 2…I) is the record number in the data set, representing the data set size, p_i is the predicted value, and x_i is the original value.

The coefficients of determination (R^2) were calculated for each calibration model: (i) fit polynomial, (ii) logarithmic curves, and actual and predicted values using the NN model generated with (iii) the first NN procedure and (iv) the second NN procedure.

RESULTS

Characterization of measurement procedures

Different circle-shaped probes were used for the characterization and measurement. Dimensions of the probes are represented in Table 1. Five different probes were used that differed in (i) diameter and (ii) thickness of the ring and formed different contact areas. It is mentionable that the measurement had both sides (top and bottom) covered with tin-plated copper. During the measurement, the bottom part of the probe contacts the liquid, but it also must be taken into account that interaction due to surface tension between the top layer and the liquid exists.

Table 1. **Dimensions of the probes used for measurements**

No.	Diameter, mm	Thickness, mm	Area, mm²	Perimeter, mm
1	10.0	1.0	28.3	56.5
2	15.0	1.0	44.0	88.0
3	15.0	2.0	81.7	81.7
4	20.0	1.0	59.7	119.3
5	20.0	2.0	113.1	113.1

Two reference solutions were measured using different diameter (d) and thickness (t) probes: (i) bidistilled water and (ii) acetone (Fig. 2). It was observed that in order to retract bigger diameter

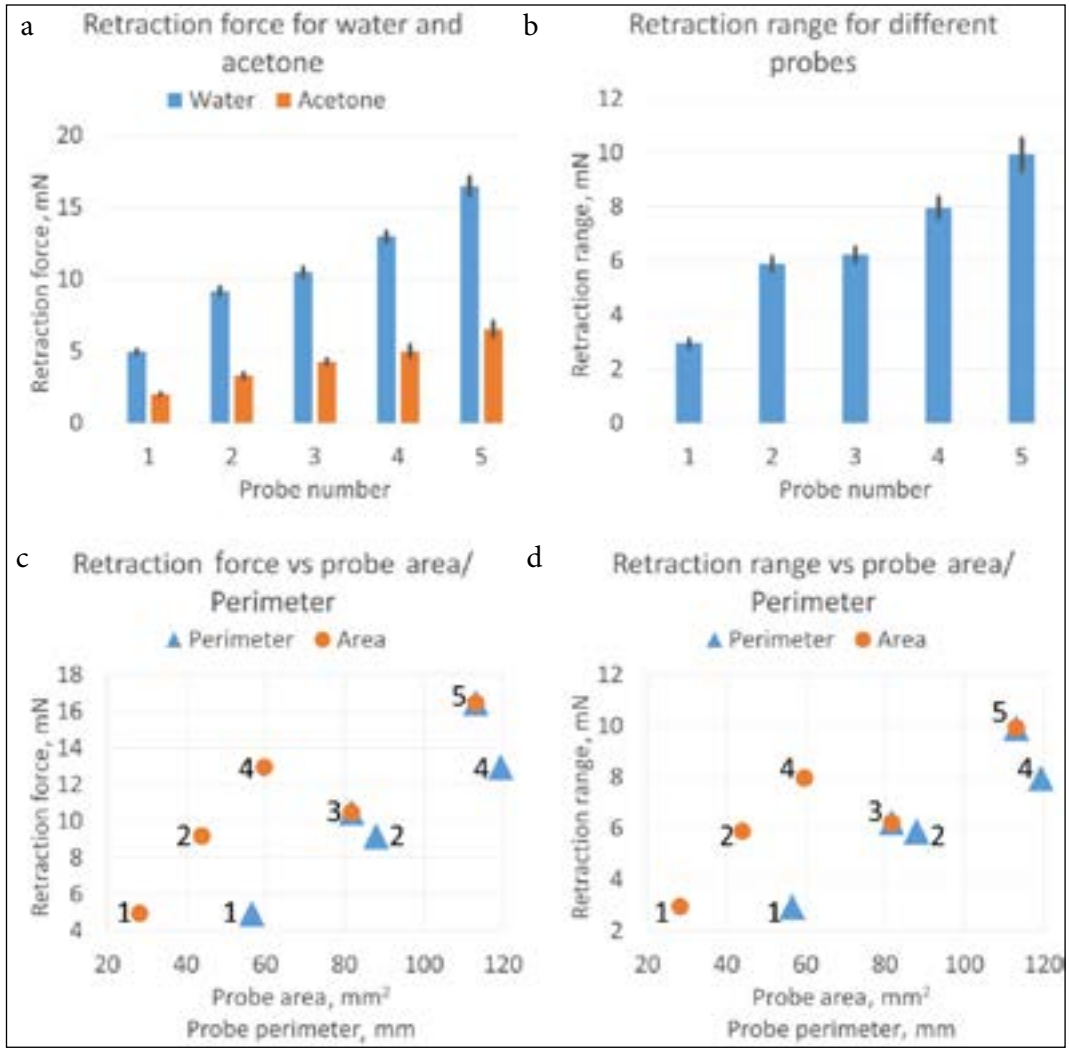

Fig. 2. Comparison of measurement parameters using different probes. (a) Retraction force for different probes measured in water and acetone. (b) Retraction range for different probes. (c) Plot representing retraction force dependency on the probe area or the probe perimeter. (d) Plot representing retraction range dependency on the probe area or the probe perimeter. Numbers indicate the probes: (1) d 10 mM, t 1 mM; (2) d 15 mM, t 1 mM; (3) d 15 mM, t 2 mM; (4) d 20 mM, t 1 mM; (5) d 20 mM, t 2 mM

probes from the surface of the liquid, a higher force (retraction force) was needed (Fig. 2a). In all cases, a lower retraction force was observed for the acetone solvent than for bidistilled water. Moreover, the measurements showed that the same diameter probes having a bigger area needed a higher retraction force (probes 2 vs 3 and 4 vs 5). For analytical instrumentation, the measurement range is important. Therefore it was decided to express it as a retraction range (mN), subtracting the retraction force value of acetone from the retraction force of water (Fig. 2b). Usually, the load cells that measure the force or other instruments with conventional sensors provide similar noise values at different levels of readings. For example, the instrument sensitivity can be increased if a higher perimeter and area probe was used for the measurement, as it was demonstrated for the designed instrument. On the other hand, cases, where minute volumes of samples are investigated, can only be solved using miniature probes (in this case, probe 1 or probe 2). This allowed reducing the sample volume down to 1 ml.

In Fig. 2c, d, the dependency between the probe areas, probe perimeters, retraction force and retraction range is represented. As demonstrated in the Figure, the dependency is complex showing high correlations: (i) the coefficient of determination (R^2) for the probe area vs retraction force was 0.78, (ii) R^2 for the probe perimeter vs retraction

force was 0.83, (iii) R^2 for the probe area vs retraction range was 0.74, and (iv) R^2 for the probe area vs retraction force was 0.86.

Later calibration, modelling and *in situ* experiments with real samples were performed using probe 2 (d 15, t 1).

Calibration and measurement of modelled solutions

Attempt to calibrate the designed instrument for the determination of detergents was performed. Fourteen different levels of SDS concentrations were measured. The range (0.005–21 672 mM) was selected so that the critical micellar concentration (8.2 mM) would be covered (Fig. 3).

It was observed that the dependency between the retraction force and the SDS concentration was too complex to generate single linear, polynomial or logarithmic fitting. It was decided to use a conditional calibration procedure. The conditional calibration covers the cases where a full range of data has to be segmented. In classical methods, the conditional calibration is usually avoided because such calculations require more computational intensity, but this is not a problem using modern-day computers. The segmented smoothing approach was demonstrated with the migration velocity-adaptive moving average method, where it was programmed into a 16 MHz 8-bit low-performance microcontroller. The conditional calibration here represents the following statements: (i) if retraction force (F) ≥ 8.5 (mN), then the calculation of concentrations should be done following the polynomial equation, and (ii) if F < 8.5 (mN), the calculation of concentrations should be done following he logarithmic equation. Here 8.5 (mN) is the cross-point of the logarithmic and polynomial curves. The polynomial equation ($y = 65187.198 \times x^2 - 895.881 \times x + 9.222$, where y is the retraction force F and x is the concentration C) represented in Fig. 3 must be transformed so that instead of y value, x should be calculated: $x = 0.00021832 \times y^2 - 0.005022 \times y + 0.02775609$. This procedure is easily calculated in the MS excel, inverting the y- and x-axis. Similarly, the logarithmic equation ($y = -1.208 \times \ln(x) - 0.065$, where y is F and x is C) must be transformed into the exponential equation: $x = 0.899737 \times e^{-0.819808} \times y$.

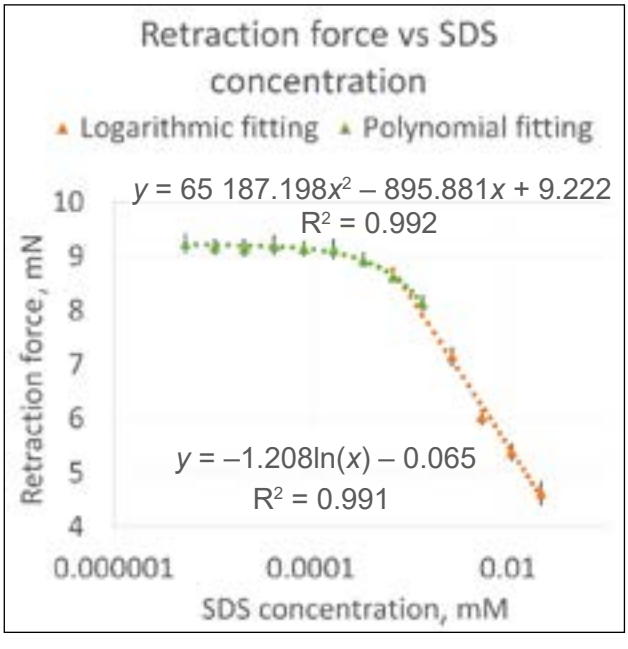

Fig. 3. Retraction force needed for different levels of the concentration of SDS

Neural networks should be considered as conditional dependency between input and output values. The developed NN model is subdivided into multiple segments representing certain ranges, where each range has its own linear equation composed of weights, inputs and outputs [21]. A mathematical model coupled to the neural networks was recently applied to solve another chemical problem – the prediction of the extraction recovery of polycyclic aromatic hydrocarbons [8].

Using two different procedures, (i) the first NN procedure and (ii) the second NN procedure, the neural network model was trained (Fig. 4). In the first NN procedure, 140 data points, with each repetition (10) at different concentration levels (14), were used. The data set was split in two similar size parts: (i) training and (ii) testing. Different combinations of hidden layers and neurons in the hidden layers were used for training. MSE corresponding to the mM concentrations of SDS was calculated for a combination of the trained neural networks. It was determined that two hidden layers, where the first and the second contained 4 neurons, showed the lowest scaled error (0.047) and absolute MSE (4.4×10^{-7}) (Fig. 4b). The training of the network took 254 steps. The coefficient of determination was calculated for the predicted and actual data of the first NN procedure trained network. R^2 was 0.986. Comparing it to the polynomial (0.992) and logarithmic (0.991) fitting coefficients, the R^2 for the first NN procedure trained

network was lower. On the other hand, the NN training procedure covers all the range of concentrations and equations generated for polynomial and logarithmic fitting are segmented into 2 ranges: (1) from 0.005 to 0.843 mM (polynomial) and (2) from 0.843 to 21.673 mM (logarithmic).

For the second NN procedure, the same combinations of hidden layers and neurons were used as in the first NN procedure training. The data set is composed of 2,000 data points and half of them was used for training, where another half was used for testing. Differently from the first NN procedure, the lowest MSE was observed for a combination of 2 hidden layers, where the first one contained 3 neurons and the second one contained 2 neurons (Fig. 4d). It took 601 steps to train the NN using the second NN procedure. For the second NN procedure trained NN, a scaled error was lower (0.0086) than for the first NN procedure trained network (0.0468). Additionally, the absolute MSE was almost two decades lower for the second NN procedure trained network (7.7×10^{-9}) than for the first NN procedure trained network (4.4×10^{-7}). The R^2 of the second NN procedure of the predicted and actual data points was 0.999 that can be considered superior to the first NN procedure trained network (R^2 of actual and predicted data points was 0.986) and superior to the model

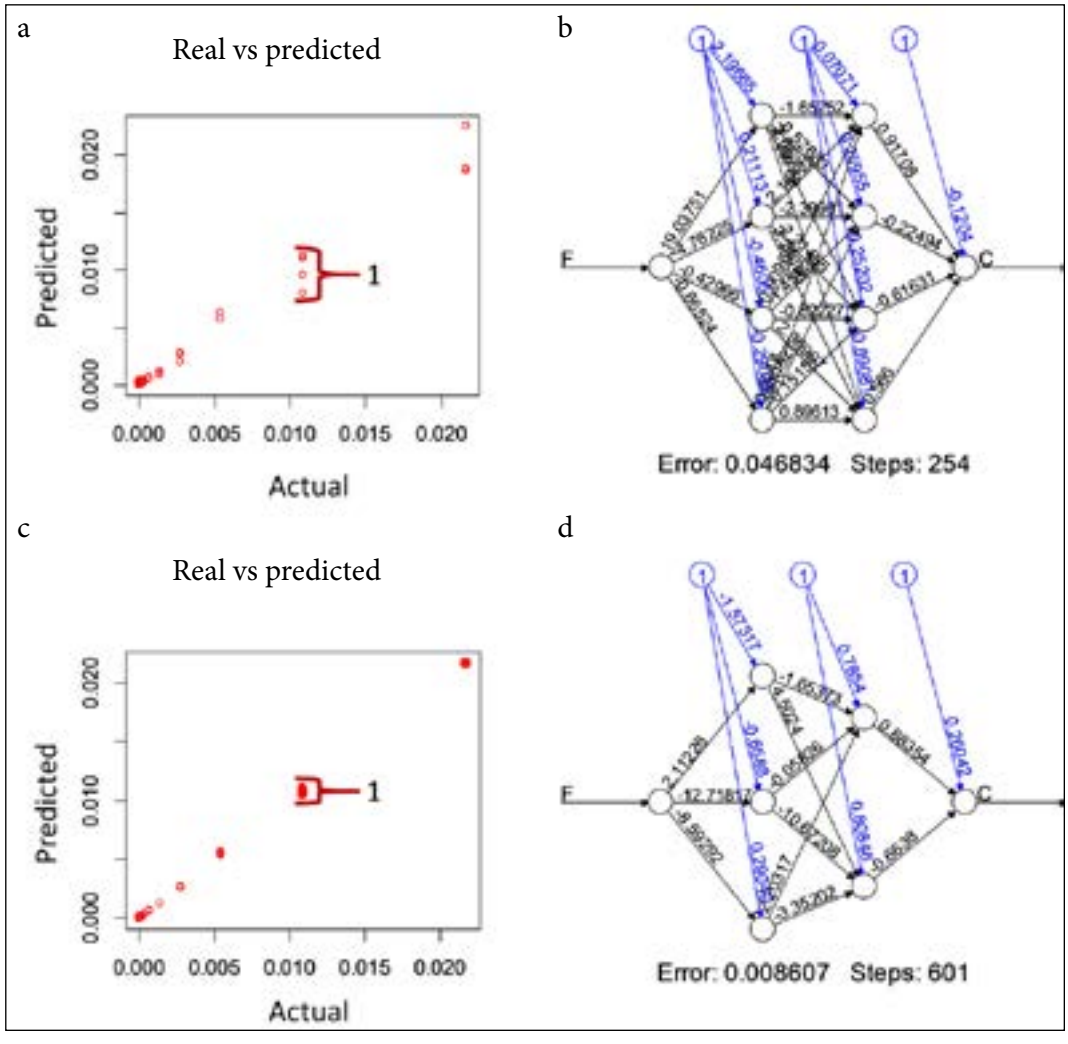

Fig. 4. Neural network models and comparison between actual and predicted concentrations. (a) Plot representing the distribution of actual and predicted concentrations of SDS when the neural network is trained using the first NN procedure. (b) Neural network model according to the first NN procedure. (c) Plot representing the distribution of actual and predicted concentrations of SDS when the neural network is trained using the second NN procedure. (d) Neural network model according to the second NN procedure. Markings: (1) representation of error near the CMC concentration of SDS, (F) force (mN) – NN input, (C) concentration of SDS (mM) – NN output

developed using a polynomial (R^2 0.992) and logarithmic (R^2 0.991) fitting.

Neural networks are a less intuitive method than linear, polynomial or logarithmic fitting methods typically used by analytical chemists. Using NN, it is difficult to draw a representative plot, similar to Fig. 3 – polynomial and logarithmic fitting of the retraction force and concentrations. On the other hand, NN models are used for numerous different fields, including life sciences, medicine, and analytical chemistry [22–24].

Neural networks is a machine learning method that is efficient with large-sized data sets [25]. In chemical analytical sciences, obtaining large-sized data sets can be problematic and expensive. As it was demonstrated, it is possible to train a neural network model using a moderate-sized data set (in this case 140 data points), where each repetition is treated as the data point. On the other hand, analysts are used to repeating a single data point from 3 to 5 times and calculating a mean, which is later used as the determined data point. The drawback of this procedure is that the size of the data set is reduced significantly and can be solved (as demonstrated in a previous study) by generating additional data points with the injected error. Such procedure requires known statistical evaluations (standard deviation, distributions, confidence intervals, etc.) of the measurements and the instrument.

Often analytical methods and instruments are calibrated using linear equations, and a drawback of such calibration is a reduced dynamic range. In electrochemical impedance spectroscopy, pseudo-linear ranges are used for the determination of chemicals [26]. In certain cases separating multivalent analytes, the calibration curve deviates from predicted concentrations at trace levels as it is known for phosphate ion applying capillary electrophoresis – contactless conductivity detection [27, 28]. In the mentioned cases, where calibration is dynamic, the range can only be increased if the proposed method of conditional calibration was used or neural network models for the prediction of concentrations were used. The proposed techniques are expected to benefit from analytical methods used in electrochemistry, photometry, spectrometry and separation science [5, 29–31].

Real sample analysis *in situ*

Real samples were analyzed: (i) modelled leftover of surfactants on the surfaces – (a) SDS on stainless steel and (b) SDS on the glass, (ii) river water – (a) Nemunas and (b) Neris, and (iii) fungal growth medium in the plateau region with (a) *I. lacteus* and (b) *P. ostreatus*. Further results are described presenting values obtained using the second NN procedure trained neural network. It was observed that more SDS was recovered from the glass (4.1 mM) than from the stainless steel surface (3.0 mM). In the Nemunas River, 2.3 mM of SDS equivalent concentration was determined, and in the Neris River 1.0 mM of SDS equivalent concentration. In

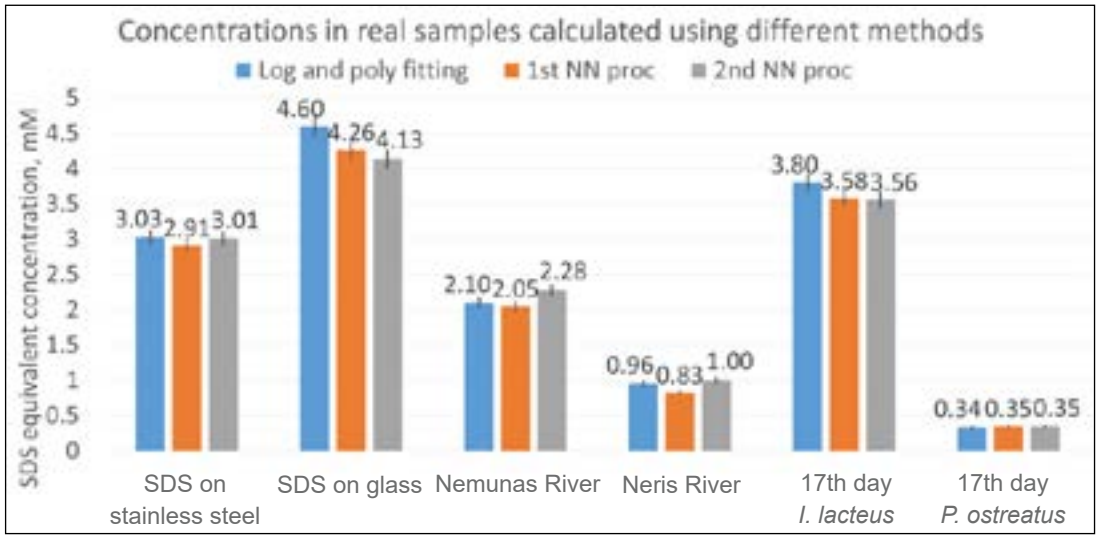

Fig. 5. Comparison of different samples and concentrations calculated using different methods. Concentrations provided as SDS equivalents in mM

the determination of the growth medium of fungi, previous results were confirmed. *I. lacteus* produced more surface tension modifying compounds than *P. ostreatus* [13]. The equivalent concentration of SDS for the *I. lacteus* growth medium was 3.6 mM, and for *P. ostreatus* it was 0.4 mM.

In Fig. 5 represented concentrations do not perfectly match. It is visible that at higher (>3.0 mM) concentrations, the conditional calibration using polynomial and logarithmic equations show slightly higher concentrations than both of the NN models predict. At lower concentrations (<3.0 mM), the results differ for different NN models. The NN model trained using the first NN procedure shows smaller values of the equivalent SDS concentration except for the last sample, which is 17th-day *P. ostreatus* growth medium. At lower concentrations (<3.0 mM), the NN model trained using the second NN procedure showed slightly higher values of the equivalent SDS concentrations.

In the future, it is planned to use the developed instruments and procedures for generating reference data and using them with the chromatographic data segmentation method for mining out exactly what substances are responsible for liquid surface tension modifying properties in biological systems and environment samples [7].

CONCLUSIONS

Portable surface tension instrumentation is characterized and applied for real sample analysis. The instrument can be calibrated using: (i) conditional calibration with polynomial and logarithmic equations, (ii) the first NN procedure neural network model trained with the dataset, where each repetition is treated as data point, and (iii) the second NN procedure neural network model trained with a data set of mean values, where additional data points are generated injecting error based on statistical information. For the second NN procedure trained neural network model, the determination coefficient was found superior compared to those of other calibration means ($R^2 > 0.999$ vs $R^2 < 0.992$). The proposed alternative calibration methods can be used with different analytical chemistry methods that require a broad range of investigated concentrations, and the dependency is dynamic.

Recommendations for the future experiments are the following: (i) applying the neural network procedure for temperature compensated readings and (ii) the investigation and design of advanced geometry probes for surface tension measurements.

Acknowledgements

This research was funded by a Grant (No. 01.2.2-LMT-K-718-01-0074) from the Research Council of Lithuania.

Received 19 July 2021
Accepted 11 August 2021

References

1. M. Kaljurand, *Trends Environ. Anal. Chem.*, **1**, e2 (2014).
2. K. R. Elkin, *J. Chromatogr. A*, **1352**, 38 (2014).
3. B. Yang, M. Zhang, T. Kanyanee, B. N. Stamos, P. K. Dasgupta, *Anal. Chem.*, **86**, 11554 (2014).
4. T. Drevinskas, L. Telksnys, A. Maruška, J. Gorbatsova, M. Kaljurand, *Electrophoresis*, **39**, 2877 (2018).
5. T. Drevinskas, A. Maruška, E. Gladkauskas, et al., *Chemija*, **29**, 209 (2018).
6. F. Postberg, N. Khawaja, B. Abel, et al., *Nature*, **558**, 564 (2018).
7. T. Drevinskas, A. Maruška, L. Telksnys, et al., *Anal. Chem.*, **91**, 1080 (2019).
8. T. Drevinskas, A. Maruška, K. Bimbiraitė-Survilienė, et al., *ACS Omega*, **6(22)**, 14612 (2021).
9. M. Lechuga, M. Fernández-Serrano, E. Jurado, J. Núñez-Olea, F. Ríos, *Ecotoxicol. Environ. Saf.*, **125**, 1 (2016).
10. J. C. Goldman, M. R. Dennett, N. M. Frew, *Deep Sea Res. Part A Oceanogr. Res. Pap.*, **35**, 1953 (1988).
11. R. J. Lee, J. R. Saylor, *Int. J. Heat Mass Transf.*, **53**, 3405 (2010).
12. W. McCance, O. A. H. Jones, M. Edwards, A. Surapaneni, S. Chadalavada, M. Currell, *Water Res.*, **146**, 118 (2018).
13. T. Drevinskas, R. Mickiene, A. Maruška, et al., *Anal. Bioanal. Chem.*, **408**, 1043 (2016).
14. N. Tiso, J. Mikašauskaitė, M. Stankevičius, et al., *Toxicol. Environ. Chem.*, **98**, 77 (2016).
15. T. Drevinskas, G. Naujokaitytė, A. Maruška, et al., *Carbohydr. Polym.*, **173**, 269 (2017).
16. T. Drevinskas, L. Telksnys, A. Maruška, J. Gorbatsova, M. Kaljurand, *Anal. Chem.*, **90**, 6773 (2018).
17. RStudio Team, *RSudio: Integrated Development for R.*, RStudio, Inc., Boston, MA (2015).
18. F. Günther, S. Fritsch, *R J.*, **2**, 30 (2010).
19. T. Drevinskas, R. R. Mickiene, A. Maruška, et al., *Anal. Methods*, **10**, 1875 (2018).
20. T. Drevinskas, R. Mickienė, A. Maruška, et al., *Chemija*, **29**, 124 (2018).
21. E. Alpaydın, *Introduction to Machine Learning*, 2nd edn., The MIT Press, London (2010).

22. D. Taylor, A. Harrison, D. Powers, *Forensic Sci. Int. Genet.*, **30**, 114 (2017).
23. M. Wesołowski, B. Suchacz, *Anal. Bioanal. Chem.*, **371**, 323 (2001).
24. J. S. Chou, N. T. Ngo, W. K. Chong, *Eng. Appl. Artif. Intell.*, **65**, 471 (2017).
25. D. Cielen, A. D. B. Meysman, M. Ali, *Introducing Data Science: Big Data, Machine Learning, and More, Using Python Tools*, 1st edn., Manning, NY (2016).
26. E. Barsoukov, J. R. Macdonald, *Impedance Spectroscopy: Theory, Experiment, and Applications*, 2nd edn., John Wiley & Sons, Inc., Hoboken, New Jersey (2005).
27. T. Drevinskas, M. Kaljurand, A. Maruška, *Electrophoresis*, **35**, 2401 (2014).
28. T. Drevinskas, A. Maruška, V. Briedis, *Electrophoresis*, **36**, 292 (2015).
29. W. R. Vandaveer IV, S. A. Pasas-Farmer, D. J. Fischer, C. N. Frankenfeld, S. M. Lunte, *Electrophoresis*, **25**, 3528 (2004).
30. F. S. Felix, L. Angnes, *Biosens. Bioelectron.*, **102**, 470 (2018).
31. T. Drevinskas, M. Stankevičius, K. Bimbiraitė-Survilienė, et al., *Electrophoresis*, **39**, 2425 (2018).

Tomas Drevinskas, Jūratė Balevičiūtė, Kristina Bimbiraitė-Survilienė, Gediminas Dūda, Mantas Stankevičius, Nicola Tiso, Rūta Mickienė, Domantas Armonavičius, Donatas Levišauskas, Vilma Kaškonienė, Ona Ragažinskienė, Saulius Grigiškis, Enrica Donati, Massimo Zacchini, Audrius Maruška

NEŠIOJAMO SKYSČIŲ PAVIRŠIAUS ĮTEMPIMO MATAVIMO PRIETAISO, VEIKIANČIO PER NEURONŲ TINKLUS, KŪRIMAS IR TAIKYMAS

S a n t r a u k a

Šiame darbe aprašytas nešiojamas paviršiaus įtempimą matuojantis instrumentas, pateikta jo charakteristika ir pademonstruotas pritaikymas. Prietaisas veikia belaidžiu būdu ir gali matuoti bandinius *in situ*. Turi keičiamus skirtingų dydžių matavimo zondus, kuriais galima matuoti bandinius nuo 1 iki 10 ml. Atitraukimo jėgos ir surfaktanto koncentracijos ryšys yra sudėtingas, todėl šiame darbe buvo pasiūlyti du kalibravimo metodai: 1) sąlyginė kalibracija pritaikius polinominę ir logaritminę funkcijas, 2) surfaktanto koncentracijos spėjimas pritaikius apmokytą neuroninių tinklų modelį. Apmokytas neuroninių tinklų modelis pademonstravo aukštą determingumo koeficientą (0,999), o sąlyginė kalibracija – šiek tiek mažesnius determingumo koeficientus. Polinominė funkcija atitiko 0,992, o logaritminė – 0,991 determingumo koeficientą.